Engineering Geology 229 (2017) 1–12

Contents lists available at ScienceDirect

Engineering Geology

journal homepage: www.elsevier.com/locate/enggeo

Impact of land subsidence due to residual gas production on surficial infrastructures: The Dosso degli Angeli field study (Ravenna, Northern Italy)

Umberto Simeoni[a], Umberto Tessari[a], Corinne Corbau[a,*], Omar Tosatto[b], Paolo Polo[c], Pietro Teatini[d]

[a] Dipartimento di Fisica e Scienze della Terra, Università degli Studi di Ferrara, Via Saragat 1, 44121 Ferrara, Italy
[b] M3E Srl, Via G. Morgagni, 44, 35121 Padova, Italy
[c] Hydro-Nova, Preganziol, Italy
[d] Dept. of Civil Environmental and Architectural Engineering, University of Padova, Via Marzolo, 9, 35131 Padova, Italy

ARTICLE INFO

Keywords:
Land subsidence
Differential displacements
Hydrocarbon production
Vulnerability of coastal areas

ABSTRACT

The Dosso degli Angeli reservoir is located along the coast of the Adriatic Sea, approximately 20 km north of Ravenna, Italy, in the nearby of the Comacchio Lagoons. The field was discovered in 1968 and the production started in 1971. The production strongly decreased from 1998 to 2004 and suspended in 2004. In 2012 Eni, the oil company managing the reservoir, has planned to complete the exploitation of the residual reserves over the period from 2013 to 2023. An elasto-plastic FE model provided by Eni was used to measure the expected residual land subsidence, whose maximum value will amount to 2.8 cm. In this work the environmental impact assessment of the expected land subsidence has been quantified on the lowlying coastland above the reservoir. Initially, the subsidence map has been used to quantify the displacement gradient ξ in correspondence of sensitive structures (bridges, pumping stations, lagoon embankments, historical buildings, power plants and a power lines) in order to assess the possible damages. Because the maximum ξ value amount to 1×10^{-5}, i.e. 1 mm over 100 m, no damage is expected to the structures. Moreover, hydrological (HEC-HMS) and hydraulic (HEC-RAS) models have been used to evaluate the possible effects of the land subsidence on the efficiency of the main drainage networks used to keep dry the area, which is mainly located below the mean sea level. The results have shown a negligible loss of efficiency of the drainage system. The study allows concluding that land subsidence due to the residual gas production from the Dosso degli Angeli reservoir will not affects the environment, hydraulic safety, and infrastructures of the Comacchio Lagoons and the lowlying coastland surrounding this precious natural environment.

1. Introduction

Relative sea level rise (RSLR), i.e., the superposition of eustatic rise of the sea and land subsidence, represents one of the geologic hazards threatening low-lying coastlands worldwide (Nicholls et al., 1999, 2008). One of these zones is the wide flat plain around the Po River delta, northern Italy, where the study area is located. This coastal region is characterized by the presence of a significant historical heritage (e.g., Ravenna), recreational villages known all over Europe (e.g., Rimini), industrial centers and harbors (e.g., the Ravenna port, the most important one in the Adriatic Sea for merchandise traffic), natural environments such as lagoons, marshes, and reclaimed farmlands generally lying below the mean sea level and kept dried by a dense network of reclamation channels and pumping stations (Fig. 1). This area is the one at greatest risk in Italy (Bondesan et al., 1995a) since the combined effect of land subsidence and eustatic sea level rise produced a loss of land elevation with respect to the mean sea level ranging from centimetres to meters over the last decades, and created a significant ecological and environmental impact (Bondesan and Simeoni, 1983; Teatini et al., 2005; Simeoni and Corbau, 2009; Tosi et al., 2009). The entire area has experienced permanent changes in coastal morphology and morphodynamics, which have caused temporary effects such as beach erosion, wave setup, flooding, and sea encroachment (Gambolati et al., 1999).

In this wide and complex area, land subsidence is characterized by a highly variable distribution with several natural and anthropogenic factors controlling land motion (Simeoni and Bondesan, 1997; Carminati and Martinelli, 2002; Bitelli et al., 2010). They act on

* Corresponding author.
E-mail addresses: g23@unife.it (U. Simeoni), tssmrt@unife.it (U. Tessari), cbc@unife.it (C. Corbau), o.tosatto@m3eweb.it (O. Tosatto), p.polo@hydronova.tech (P. Polo), pietro.teatini@unipd.it (P. Teatini).

http://dx.doi.org/10.1016/j.enggeo.2017.09.008
Received 23 February 2017; Received in revised form 27 July 2017; Accepted 8 September 2017
Available online 11 September 2017
0013-7952/

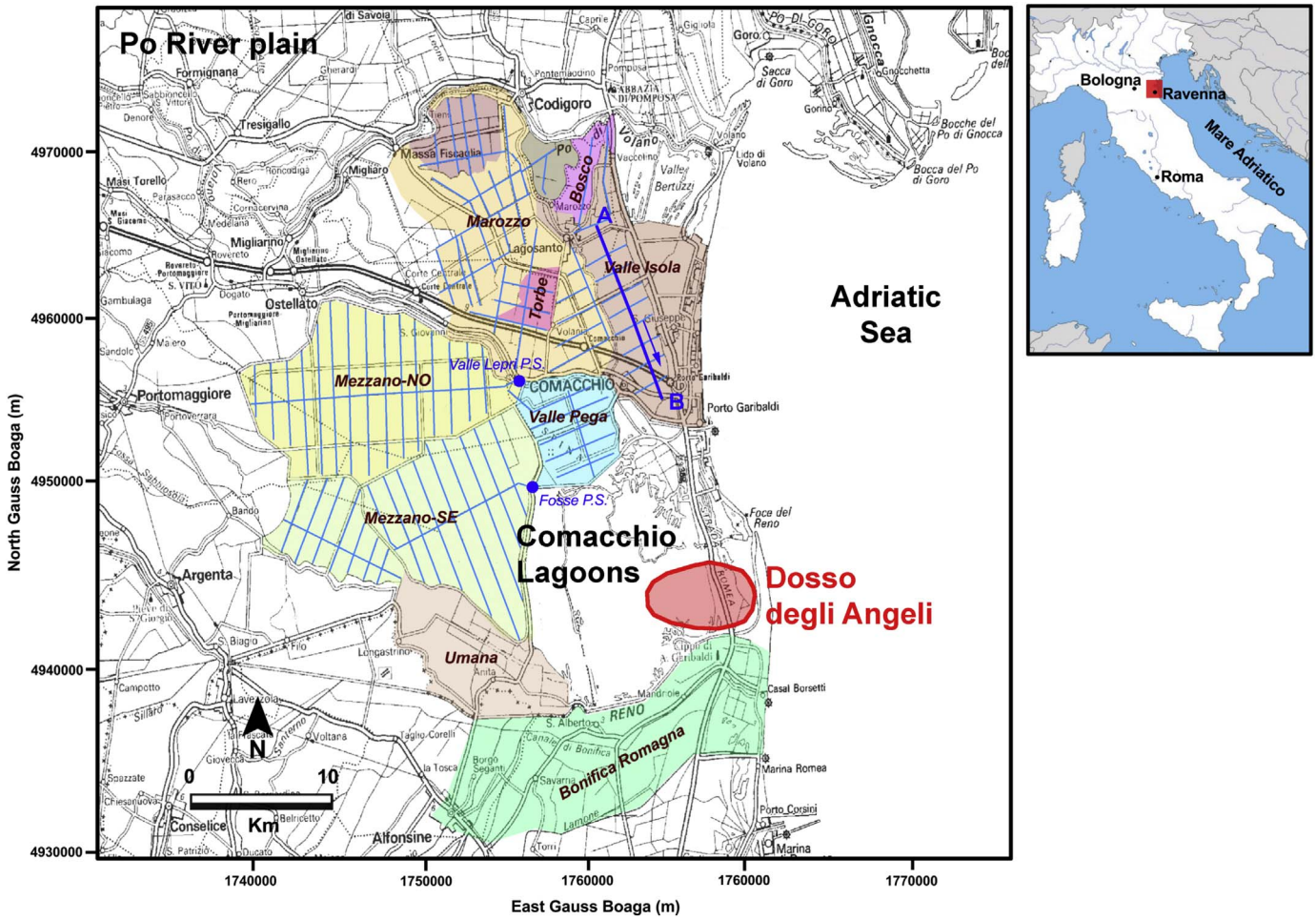

Fig. 1. Map of the study area with the trace of the Dosso degli Angeli reservoir (in red). The reclamation basins and the main drainage networks simulated by the HEC-HMS and HEC-RAS models are highlighted. The main pumping stations (P.S.) and the trace of the Valle Isola channel (Fig. 13) are also shown (in blue). (For interpretation of the references to colour in this figure legend, the reader is referred to the web version of this article.)

different depth ranges, areas and timescales (from millions to thousands of years and hundred to tens of years, respectively), thus reflecting the geological history and the human development of the territory (Carminati and Di Donato, 1999; Tosi et al., 2009).

Anthropogenic land subsidence due to the production of subsurface fluids (oil, gas, or water) has been observed worldwide over the last decades. Aquifer over-exploitation produced severe land subsidence, for example, in Mexico City (Ortiz-Zamora and Ortega-Guerrero, 2010), Shanghai and Beijing in China (Wu et al., 2010; Zhu et al., 2015), San Joaquin Valley in USA (Galloway and Riley, 1999), Jakarta in Indonesia (Ng et al., 2012). Well-known examples of subsidence above compacting hydrocarbon fields are, for example, those at Long Beach, California (Colazas and Strehle, 1995), in Venezuela (Finol and Sancevic, 1995), or the Ekofisk field in the North Sea (Hermansen et al., 2000).

Short-term anthropogenic causes became a key problem for the land stability of the whole northern Adriatic coastland during the twentieth century, especially from the World War II to the end of the 1960s when the civil, industrial, agricultural and tourist developments required huge amounts of water and an increasing of energy supply. Artesian waters were withdrawn in the Venice area (Tosi et al., 2009), gas-bearing water in the Po Delta (Caputo et al., 1970), and both groundwater and gas (inshore and offshore) in the Ravenna region (Carbognin et al., 1984; Gambolati et al., 1991; Teatini et al., 2006). The anthropogenic land subsidence contributed differently to the RSLR along the northern Adriatic coast (Fig. 2a). Since the 1980s Ravenna has been reported among major worldwide areas of anthropogenic land subsidence due to subsurface fluid removal (Carbognin et al., 1984; Gambolati and Teatini, 2015). Precise geodetic measurements indicate that the ground surface has subsided by > 1 m in some parts of the area since the early 1950s (Teatini et al., 2005).

The impacts of land subsidence on the natural, rural, and urban environments are multiple. The loss of land elevation can reduce the freeboard of embankments and ports, increasing the flood frequency and the marine storm intensity, with severe damages to urban heritages, economical activities, lagoon and coastal morphologies (Douben, 2006; Allison et al., 2016). Structural and environmental hazards can include damage of bridges, buildings, roads, gas/water pipes and underground telecommunication optical cables, failure of well casings, and increasing risk of inland sea water intrusion (Pauw et al., 2012; Erban et al., 2014). Differential land subsidence can alter the natural river and channel flow directions, inhibit discharge towards the sea with pumping stations requiring a greater head (d'Angremond and van de Water, 2012), disrupt surface drainage, reduce aquifer system storage (Hoffmann et al., 2003), create ground fissures (Carreon-Freyre et al., 2016).

The aim of the study is to evaluate the possible impact of the anthopogenic land subsidence due to the exploitation of residual hydrocarbon reserve from the Dosso degli Angeli gas field, located on the northern Adriatic coast, approximately 20 km north of Ravenna. The possibility of investigating the effects of land subsidence due to hydrocarbon production is less frequent than the cases caused by aquifer exploitation (e.g., Hung et al., 2012; Mahmoudpour et al., 2016). The investigation lasts the period from 2013 to 2023. After an overview of the geomorphological setting of the study area and a summary of the

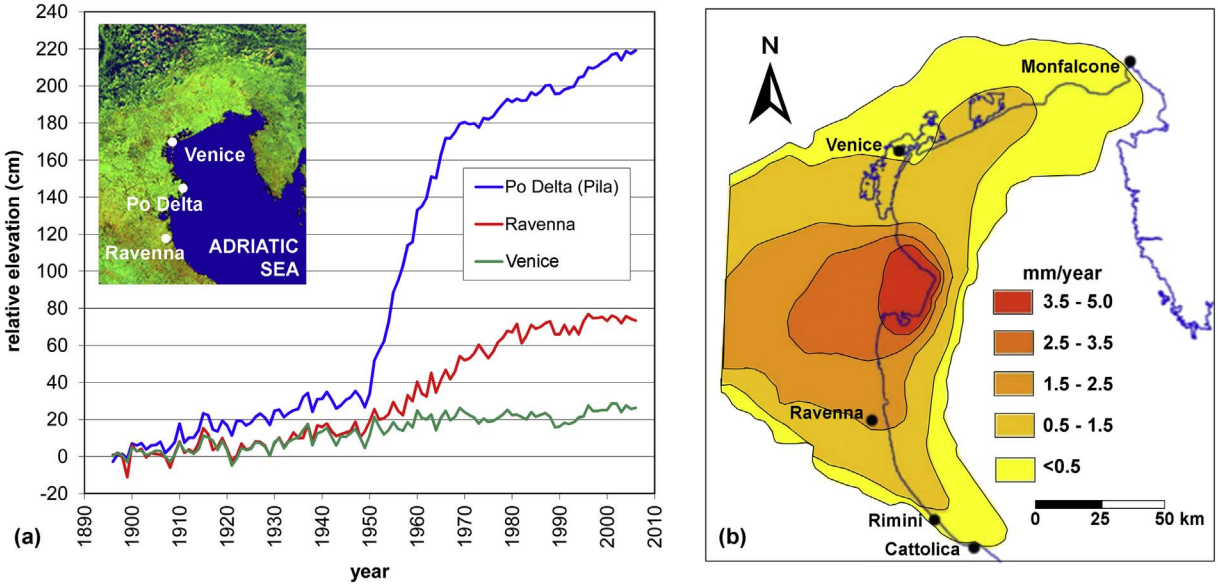

Fig. 2. (a) Relative sea level rise (RSLR) at Venice, the Po River delta, and Ravenna along the northern Adriatic coast over the period 1896–2007 (redrawn after Carbognin et al., 2011). (b) Recent natural land subsidence in the northern Adriatic coastal area (after Gambolati and Teatini, 1998). The blue line represents the shoreline of the Adriatic Sea. (For interpretation of the references to colour in this figure legend, the reader is referred to the web version of this article.)

land subsidence measured in the past decades, the main information about the geological features of the Dosso degli Angeli reservoir and its production history is provided. The land subsidence and displacement gradient expected over the reference time interval are presented. Finally, their possible effects on the hydraulic network and the main structures and infrastructures distributed in the coastal region above the reservoir are evaluated.

2. Environmental and geological setting of the study area

2.1. Geomorphological setting

The study area represents the easternmost part of the Po River plain (Fig. 1). Because of the presence of the Comacchio Lagoons, the European Union recognized this zone as a Site of Community Importance (SIC) and a Special Protection Area (ZPS). The reclamation of this coastland, which was completed in 1964, made available 18,000 ha for crop activities. The farmland is characterized by a flat topography crossed and kept drained by a large number of artificial channels controlled by pumping stations. A large number of embankments bounds the rivers and the reclaimed ponds.

From the lithological point of view, the land is characterized by alternations and interdigitation of continental and marine facies accounting for the complex evolution history. Silty-clay soils and soils rich in organic matter (peat) are largely distributed in the north-western part. Eastward, close to the coastline, fine sands and silty-sands represent the most frequent lithology (Bondesan et al., 1995b). The land elevation ranges between − 2 and + 4 m above the mean seal level (msl), with the highest zones in correspondence of sandy paleo-river beds and paleo-dunes. Peatlands are characterized by the lowest elevation because of land subsidence due to oxidation of organic matter, which has been quantified in 10–20 mm/year close to the Venice Lagoon, i.e. a few tens of km to the north of the study area (Zanello et al., 2001).

The zone is mainly devoted to crop production, with a few small villages scattered thorough the farmland. Comacchio is the main urban center and is characterized by the presence of an important historical monument known as of “Trepponti di Comacchio”, which is a masonry bridge dated 1638. Major infrastructures are related to the reclamation and drainage of the area: the Valle Lepri and Fosse pumping stations, which rise the drainage waters to a higher level than the msl, several channels, the so-called “Agosta” embankment bounding the Comacchio Lagoons. Other relevant structures are a couple of large bridges crossing the Reno River, a north-south high-voltage power-line, and the Teodora power-plant at the southernmost tip of the study zone (see Fig. 14 for their location).

2.2. Land subsidence

Land subsidence in the coastland of the Po River plain is due to the superposition of natural processes and anthropogenic activities. Natural land subsidence is also largely variable (Fig. 2b), depending on the thickness of the Plio-Quaternary deposits, the deposition age and type of the Holocene sediments, and deep tectonics (Bartolini et al., 1983; Gambolati and Teatini, 1998). Foraminiferal markers (Hyalinea balthica) and backstripping techniques on stratigraphic information from approximately 200 deep wells have been used by Carminati and Di Donato (1999) to quantify the average subsidence rate over the last 1.43 Myr. In the area of Dosso degli Angeli, they evaluated an average natural subsidence of 2 mm/year, with 0.5 mm/year caused by the compaction of the Quaternary deposits, 0.4 mm/year due to the sedimentary load, and 1.1 mm/year due to tectonics. Concerning the anthropogenic land subsidence, this is usually much larger than the natural component in the coastal part of the Po River plain and is caused by aquifer overexploitation, peat oxidation and, more locally, the development of hydrocarbon reservoirs (Carbognin et al., 1984; Teatini et al., 2006).

Several public authorities and private companies have been involved in the measurement of land subsidence in this area. The Environmental Agency of the Emilia-Romagna Region (ARPA-ER) published a first comprehensive map of the average subsidence rate in the whole region by interpolating the levelling surveys carried out between 1970/93 and 1999 (Bitelli et al., 2000). The subsidence averaged 10 mm/year in the study area, with an increase up to 20 mm/year in the northernmost tip of the Ravenna coastland where the Dosso degli Angeli is located (Fig. 3). The land subsidence measured by ARPA-ER on a levelling benchmark in the surrounding of the production wells totaled 360 mm between 1984 and 2005, with a rate of 18 mm/year and 13 mm/year over the periods from 1987 to 1999 and between 1999 and 2005, respectively.

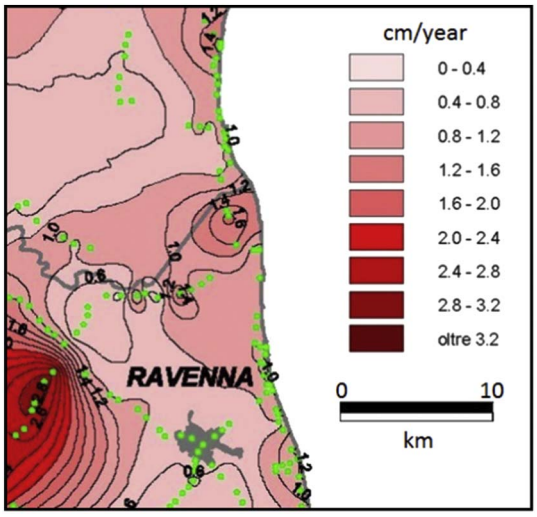

Fig. 3. Map of the subsidence rate (cm/year) built-up using the levelling surveys carried out over the period 1970/93–1999 (modified after Bitelli et al., 2000). The green dots represent the benchmark locations. (For interpretation of the references to colour in this figure legend, the reader is referred to the web version of this article.)

Levelling was also been carried out by the Municipality of Ravenna. Of interest are the surveys performed in 1986, 1992, and 1998 with the displacement values obtained over those periods shown in Fig. 4. The maximum settlement amounted to 12 to 15 mm/year close to the trace of the reservoir and significantly reduced southward.

Taking advantage of the large experience developed worldwide, for example in USA (Riley, 1986; Buckley et al., 2003) and China (Wu et al., 2008), Eni, the Italian oil company managing the reservoir, established in 1997 an extensometer station in correspondence of the production wells (see Fig. 4a for the location) to quantify the fraction of the total subsidence caused by the compaction of the shallower deposits. In particular, the station is made of two rod extensometers 30 m and 336 m deep to provide the compaction of the Holocene and the Quaternary portion where the pumped fresh-water aquifers are located, respectively. The extensometers are characterized by a sub-millimeter accuracy. The measurements shown in Fig. 5a highlight an average compaction rate of the Quaternary equal to 1.1 mm/year, which represents an evaluation of this contribution more reliable for the study area than the value 0.5 mm/year estimated by Carminati and Di Donato (1999).

Moreover, Eni accomplished the extensometer station by a continuous GPS (CGPS) in 2002. Fig. 5b provides the vertical displacements recorded until 2011. The subsidence rate decreased from 12 mm/year in 2002 to 5 mm/year in 2008.

More recently, Synthetic Aperture Radar (SAR)-based methodologies have been widely used to quantify the displacements caused by fluid production from the subsurface (Rohmer and Raucoules, 2012; Motagh et al., 2017). In the study area, ascending and descending images acquired by ERS-1/2, RADARSAT, and COSMO-SKYMED over the periods 1992–2000, 2003–2010, and 2008–2011, respectively, have been processed by the SqueeSAR (Ferretti et al., 2011) and properly combined (Tamburini et al., 2010) to quantify the vertical movements of radar targets scattered on the coastland. Because SqueeSAR provides differential displacements, it has been elected to use the 1992–1998 levelling and the CGPS records to calibrate the SqueeSAR measurements. The SqueeSAR results from the three satellites are shown in Fig. 6. The maps point out the variability of the observed displacements as a result of the various processes (surficial loads in newly urbanized zones, groundwater pumping, natural compaction of Holocene deposits, development of the Dosso degli Angeli reservoir, peat oxidation) contributing to the total subsidence. Notice that a signal of the contribution of gas production to the total subsidence is clearly distinguishable only over the period between 1992 and 2000, i.e. from ERS-1/2, when the cumulative settlement above the trace of the reservoir amounted to > 10 mm/year.

This dataset has been used to calibrate the geomechanical model over the period 1986–2011. Notice that, to remove the contribution due to the processes not connected to gas production, the measured subsidence rates have been reduced by 2.6 mm/year, that is the sum of 1.5 mm/year due to natural deep processes as estimated by Carminati and Di Donato (1999) and 1.1 mm/year due to shallow compaction and aquifer exploitation as provided by the extensometer.

3. The Dosso degli Angeli reservoir: geological setting and production history

Similar to other hydrocarbon reservoirs in the northern Adriatic sedimentary basin, Dosso degli Angeli is composed by a number of gas-bearing pools located approximately along the same vertical and

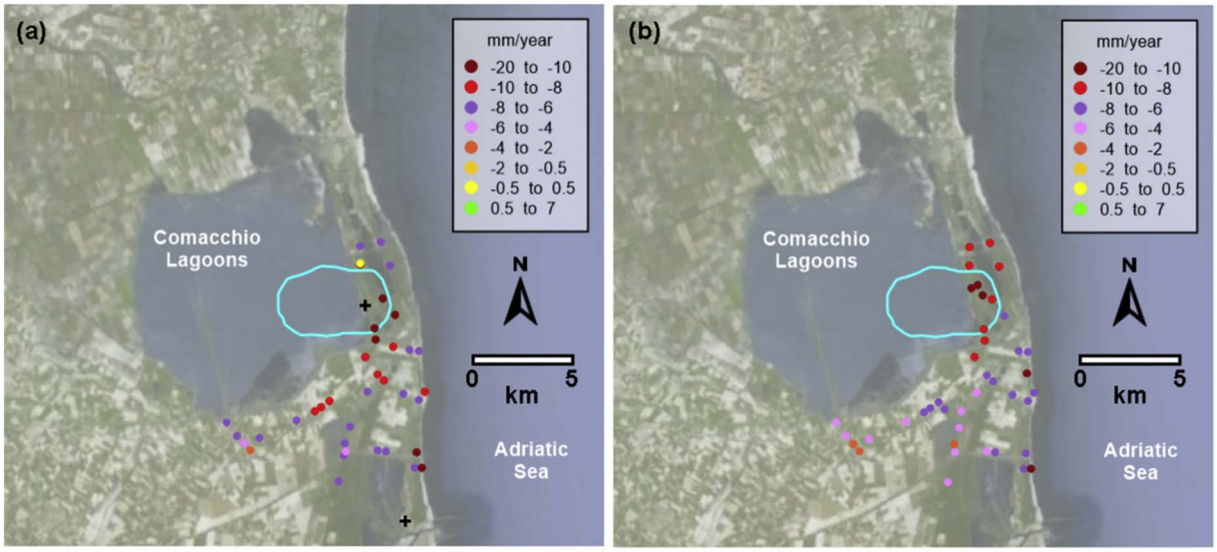

Fig. 4. Land displacement on the benchmarks of the Ravenna municipality network over the periods (a) 1986–1992 and (b) 1992–1998. Negative values mean subsidence. A light-blue line shows the trace of the Dosso degli Angeli reservoir. A black cross in (a) shows the location of the extensometer and CGPS station established by Eni. (For interpretation of the references to colour in this figure legend, the reader is referred to the web version of this article.)

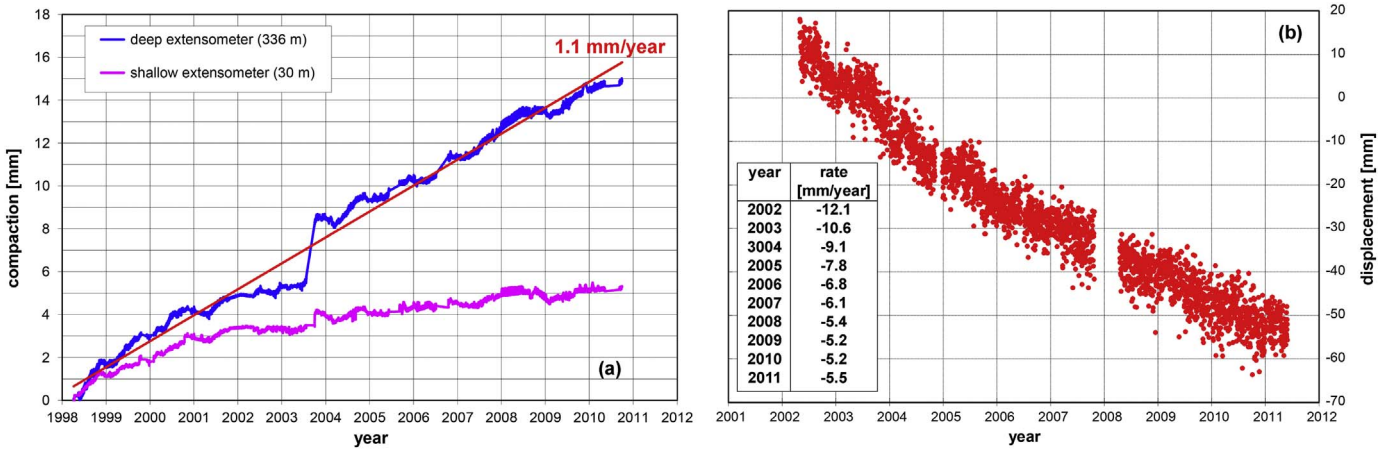

Fig. 5. Time behavior of (a) the compaction and (b) the subsidence recorded by the two extensometer and the CGPS station established by Eni above the Dosso degli Angeli reservoir. The average rates are negligibly affected by the gap occurred between 2005 and 2007.

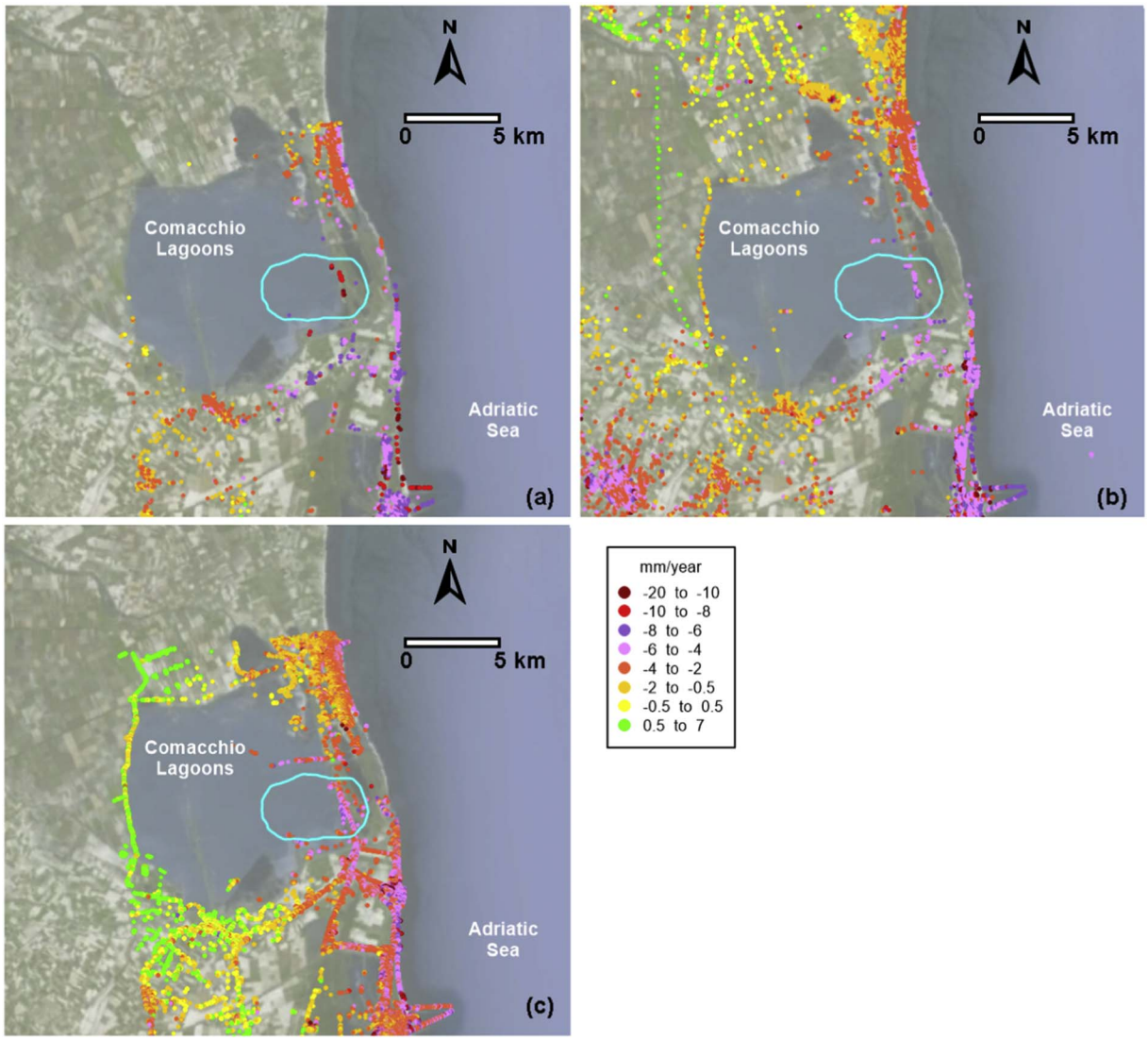

Fig. 6. Average vertical displacements (mm/year) over the periods (a) 1992–2000, (b) 2003–2010, and (c) 2008–2011 obtained by SqueeSAR on ERS-1/2, RADARSAT, and COSMO-SKYMED, respectively. Negative values mean subsidence. The trace of the reservoir is also shown.

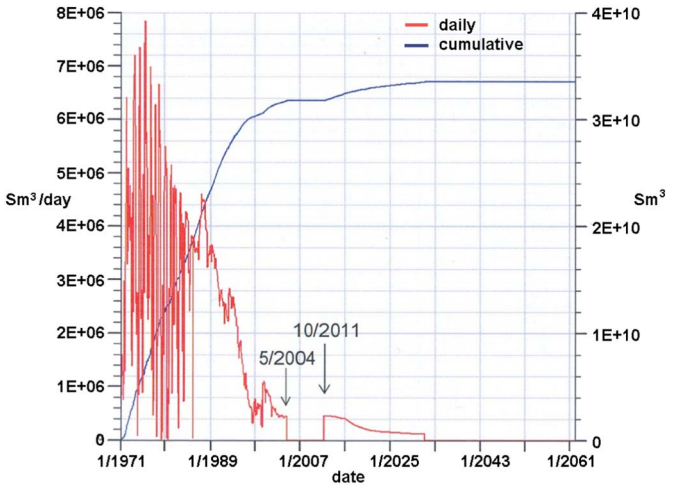

Fig. 7. Daily and cumulative gas production from the Dosso degli Angeli reservoir.

independent from the hydraulic point of view. The reservoir is formed by a structural trap with a gentle trangressive Pliocene anticline on a Miocene monocline rising north-eastward. Gas accumulation occurs in thick sandy middle- and late-Pliocene levels sealed on top by deep-marine shales and impermeable sandstone (Mattavelli et al., 1983).

Dosso degli Angeli is made of 8 pools with the gas-water-contact spanning the depth range between 2885 and 3839 m below msl and with an initial pore pressure from 318 to 504 bar. Each pool is connected to a bottom and lateral aquifer extending mainly to the north-east. The aquifers are bounded by a regional fault south-westward. The reservoir was discovered in 1968 with a gas-originally-in-place (GOIP) equal to 37×10^9 Sm^3. The production started in 1971 and temporarily closed in 2004 with a cumulative extracted volume equal to $\sim 32 \times 10^9$ Sm^3 (Fig. 7), i.e. 94% of the recoverable resources. The initial pressure p_i decreased by 65–85% depending on the pool in 1998–2004, followed by a certain recovery after the well closure due to groundwater inflow from the surrounding aquifers.

The environmental impact assessment presented in this work is focused on the residual production Eni has started in October 2011 (Fig. 7). Based on an agreement with the public environmental authorities managing the area, a further gas volume equal to about 1.8×10^9 Sm^3, which corresponds to approximately 5% of the recoverable resource, will be produced before December 2023 if it is shown that the expected land subsidence will caused a negligible impact on the coastal area. The residual production will occur from three levels, with a further pressure decline ranging from 5 to 20%p_i.

4. Materials and methods

4.1. Geomechanical model

Eni has made available the outcomes of a three-dimensional (3D) finite-element (FE) elasto-plastic geomechanical model of the Dosso degli Angeli reservoir (Ferronato et al., 2012). The model domain has an areal extent of 70 × 80 km centered on the reservoir and is confined by the ground surface above, with a 4 to 8 km deep rigid bottom corresponding to the top of the carbonates. Standard conditions with zero displacement on the outer and bottom boundaries are prescribed, while the land surface is a no-stress boundary. The 3D mesh is formed by 962′180 nodes and 5′684′055 tetrahedra (Fig. 8), with the element characteristic size ranging between 50 m above the reservoir to 2000 m along the domain boundary, thus allowing an accurate reconstruction of the subsidence bowl above the study area. The layers where the reservoir and the surrounding aquifers are located and the faults bounding the deep formation southwestward are properly discretized.

The simulations were carried out by the code GEPS3D (Janna et al., 2012) using as input data the pressure evolution computed by a fluid-dynamic production model developed by Eni using Eclipse (Schlumberger Ltd, 2007). Consistently with the Eclipse simulations, a proper constitutive relationship based on the outcome of the radioactive marker technique and linking the rock compressibility to depth and effective stress (Baù et al., 2002; Hueckel et al., 2005) was used in GEPS3D. The geomechanical model was calibrated using the subsidence measurements, properly corrected to remove the components not related to gas production, and then used to forecast the expected land displacements over the period 2013–2023.

4.2. Hydrologic and hydraulic models

Because of the low elevation of the area, land subsidence can potentially impact on the complex network of ditches and pumping stations that discharge the drainage water into the Adriatic Sea or the Comacchio Lagoons. A specific hydrologic and hydraulic modeling study was performed to check the possible loss of efficiency of the drainage system. The model domain and the main drainage network used in the simulations are shown in Fig. 1. The simulated area, which is composed of seven independent drainage sub-basins, comprises about 36,500 ha.

The HEC-HMS (Hydrologic Modeling System) hydrologic model (USACE-HEC, 2010) was used to compute the discharge along the main channels in each sub-basin. Among the available hydrologic methods, the exponential loss method was used to handle infiltration loss, neglecting evapotranspiration and baseflow because the most serious events occur in winter season and due to the flatness of the region. The kinematic-wave transformation method (Chow, 1959), which well adapts to reclamation basin and allows to change the system slope due to subsidence, was used to compute the runoff hydrograph and follow its downstream transformation along the channels. Due to the lack of specific information on the "udometric coefficient", i.e. the contribution of unit area of the basin to the formation of the peak discharge, the precipitation events in input to HEC-HMS were defined using the information on the characteristics of the pumping station of each sub-basin. For example, the maximum water discharge at the Fosse pumping station, whose sub-basin (known as Mezzano-SE) is one of the largest in the study area with an areal extent of 7′420 ha, amounts to $Q_w = 24\ m^3/s$. This discharge is characterized by a 25-year return period (T_r), which is the classical T_r value used by the Italian reclamation authorities to design the reclamation structures. Hence, a rainfall event with $T_r = 25$ years was generated by a trial-and-error procedure in order to obtain Q_w at Fosse using:

- a maximum time-of-travel of water t_t equal to 5 days in the Mezzano-SE sub-basin as computed by the Pasini empirical relation (Da Deppo et al., 2004); t_t varies between 1 and 5 days in the other sub-basins;
- a maximum rainfall intensity $i_m = 142.5$ mm/h as estimated for a t_t event by Todini (1990) in this zone of the Po plain;
- a sub-basin slope equal to 0.000015.

The hydraulic model of the main ditches and channels was developed using HEC-RAS (River Analysis System) by USACE-HEC (2016). The geometry of the drainage network, cross sections, and profiles of the watercourses were made available by the Water Reclamation Authorities managing the area. The main hydraulic structures, such as bridges, culvers, and inline structures were accounted for. The simulations were performed using in input the HEC-HMS results: the discharge for each sub-basin accounted for in the hydrologic model is uniformly distributed along the corresponding channel, with the control rule of the pumping station used as downstream boundary condition. A uniform value of the Manning roughness coefficient $n = 0.03\ m^{-1/3}s$ was used for all the channels. An example of the time behavior of the discharge at the closing section of each sub-basins as provided by

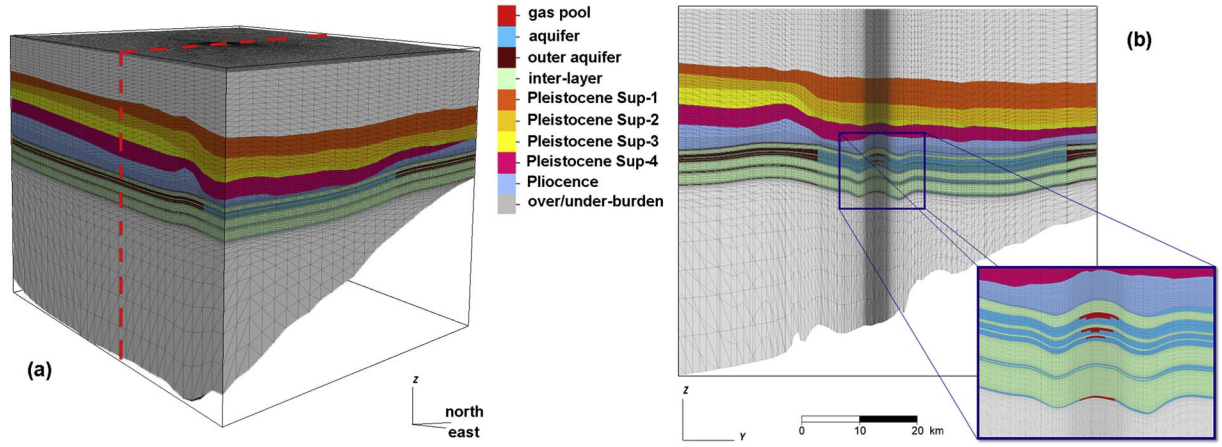

Fig. 8. (a) Perspective view of the 3D FE grid used in the geomechanical simulation of the Dosso degli Angeli reservoir; (b) north-south vertical cross section of the mesh through the dashed-red line traced in (a), highlighting the pools of the Dosso degli Angeli gas field. The colors indicate the different lithologies. The vertical exaggeration is 10 × (after Ferronato et al., 2012). (For interpretation of the references to colour in this figure legend, the reader is referred to the web version of this article.)

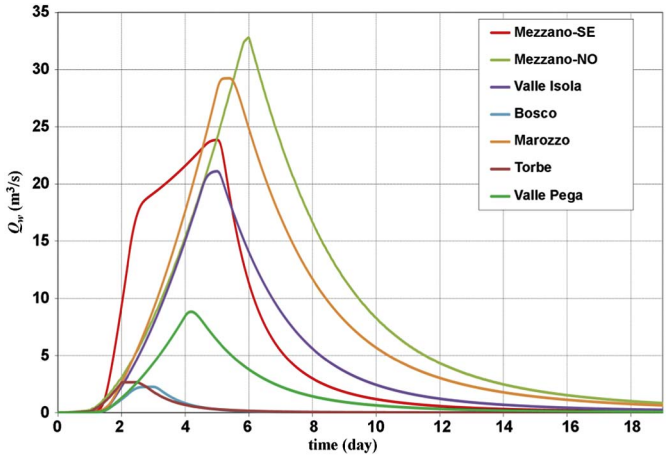

Fig. 9. Discharge hydrograph at the closing section of the various sub-basins as provided by HEC-RAS.

the hydraulic model is shown in Fig. 9.

4.3. Displacement gradients

A major concern related to land subsidence is the possible generation of differential displacements (or displacement gradient) ξ that might jeopardize the stability and integrity of the structures and infrastructures scattered in the subsiding area. Generally speaking, a rather restricted ξ is to be used wherever a criterion of aesthetic or functional nature prevails, e.g., for an important building such as a historical monument or a civil structure such as a bridge, dam, or embankment. Alternatively, a less bounding limit can be accepted for, e.g., an industrial building.

According to Bjerrum, 1963 and Ricceri and Soranzo, 1985, displacement gradients $< 1/300$, i.e. 3.33×10^{-3}, do not produce visible fissures in bearing and non-load-bearing walls. Damages to reinforced concrete structures are caused by values of ξ larger than 1/150 (6.67×10^{-3}). The most restrictive rules (Viggiani, 2003) prescribe a maximum differential displacement equal to 5×10^{-4} (1/2000) for multi-floor masonry buildings. A summary of some bounds on ξ for specific structural issues is given in Table 1.

The displacement gradient of the vertical (u_z) and horizontal (u_h) displacements at the land surface was straightforwardly computed from the outcome of the 3D geomechanical model through the relation:

Table 1
Bound of admissible displacement gradients ξ for various structural issues (after Bjerrum, 1963 and Ricceri and Soranzo, 1985.

Issue	ξ bound
Problems for the efficiency of specific machineries	1/750 (1.33×10^{-3})
Static problems for reticular structures	1/600 (1.66×10^{-3})
Absence of fissure development	1/500 (2.00×10^{-3})
Visible fissures in bearing and non-load-bearing walls	1/300 (3.33×10^{-3})
Visible tilt of tall buildings	1/250 (4.00×10^{-3})
Structural damages to reinforced concrete structures	1/150 (6.67×10^{-3})

$$\xi_i = \sqrt{\left(\frac{\partial u_i}{\partial x}\right)^2 + \left(\frac{\partial u_i}{\partial y}\right)^2} \qquad i = z, h \tag{1}$$

where x and y correspond to the west-east and south-north directions, respectively, and u_i is the vertical ($i = z$) or horizontal ($i = h$) displacement component. Notice that u_h represents the modulus of the horizontal movement calculated from the west-east and south-north components. Finally, the resultant ξ value is calculated as:

$$\xi = \sqrt{\xi_z^2 + \xi_h^2} \tag{2}$$

5. Expected land displacements and displacements gradients

The calibrated geomechanical model allows evaluating the expected land displacement and displacement gradients due to the residual production from Dosso degli Angeli.

5.1. Land displacements

Land subsidence due to the residual development of the Dosso degli Angeli reservoir is shown in Fig. 10. The shape of the subsidence bowl is elongated in the north-west - south-east direction feeling the aquifer and fault geometry, with the 1-cm isoline subsidence extending 30 km along this direction and 15 km along the orthogonal one. The maximum subsidence amounts to 2.8 cm and is expected to develop not above the reservoir but approximately 7–8 km to the north. This is due to the complex geometry of the produced layers and the contribution of the aquifer compaction to the cumulative land subsidence. Above the trace of the gas field the settlement will be < 1.5 cm. In term of subsidence rates, the contribution of the reservoir development will be < 2.8 mm/year. A qualitative evaluation of the importance of these amounts can be simply performed by their comparison with the subsidence rates recently measured in the area (Fig. 6).

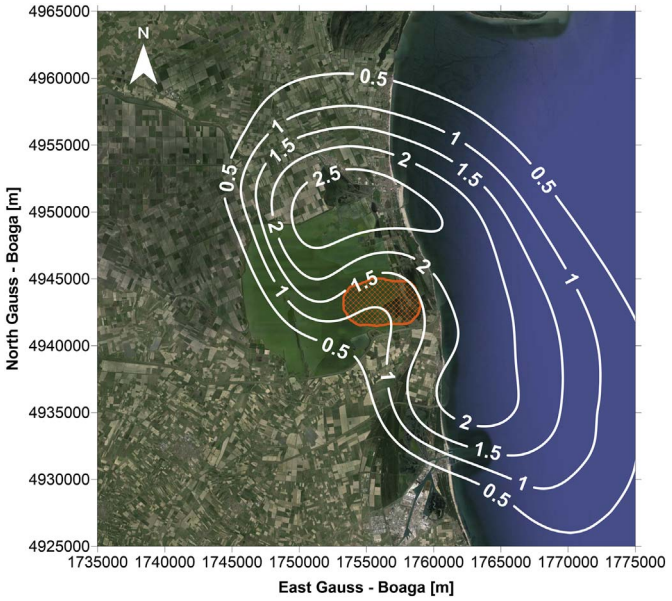

Fig. 10. Expected land subsidence (cm) due to the residual production from the Dosso degli Angeli reservoir between 2013 and 2023. The trace of the gas field is highlighted.

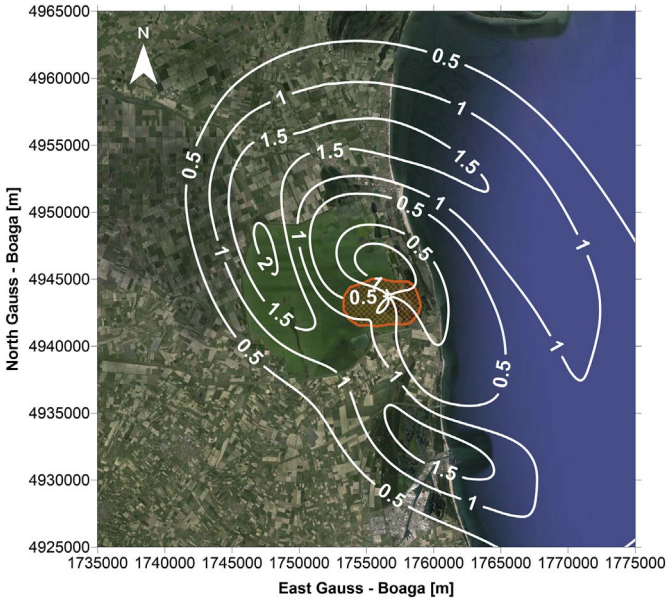

Fig. 11. Modulus of the expected horizontal displacement (cm) due to the residual production from the Dosso degli Angeli reservoir between 2013 and 2023. The trace of the gas field is highlighted.

Because of the significant depth of the reservoir, the displacement field caused by the gas production is characterized by a significant tridimensionality (Geertsma, 1973). This means that also the horizontal displacements cannot be negligible at the land surface. The 3D geomechanical model provides a quantification of this displacement component. Fig. 11 shows the modulus of the expected horizontal movement over the study decade. The computed value is generally < 1 cm with the maximum, which amounts to 2 cm, located within the Comacchio Lagoons, approximately 8 km to the north-west of the trace of the reservoir. As expected, the horizontal displacement almost vanishes close to the production wells. The shape of horizontal displacement resamples that of land subsidence.

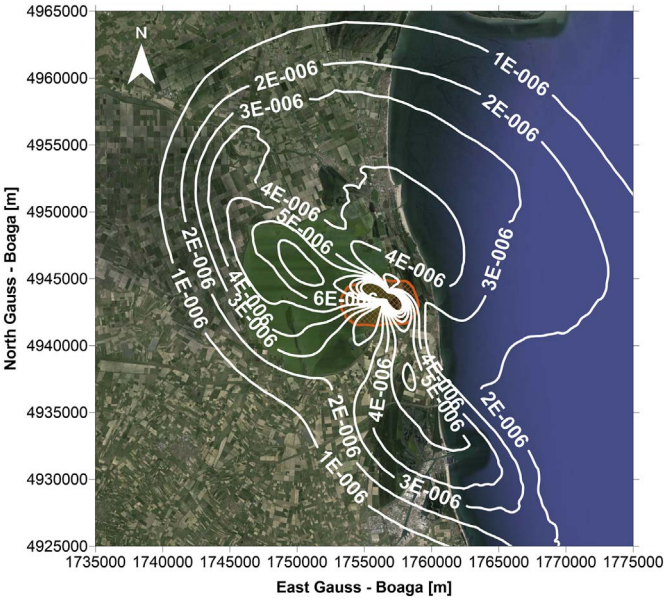

Fig. 12. Expected differential displacements due to the residual production from the Dosso degli Angeli reservoir between 2013 and 2023. The trace of the gas field is highlighted.

5.2. Displacement gradients

The displacement field provided by the 3D geomechanical model have been properly processed by Eqs. (1) and (2) to compute the expected gradient of the displacement. The outcome is shown in Fig. 12. The values range between 10^{-6} and 10^{-5}, i.e. from 0.1 to 1 mm over 100 m. The large majority of the coastland will experience an amount $< 5 \times 10^{-6}$, with the larger values located above the trace of the reservoir as mainly related to the sharp variation of the horizontal displacements.

6. Geomechanical effects on the coastland

6.1. Hydrologic and hydraulic impacts

Land subsidence can affect the efficiency of the reclamation network used to maintain the watertable below the ground surface. In particular, a change in the slope of a basin or a channel modifies the maximum travel time, the lowering of the inlet shaft of a drainage pumping station with respect to the mean sea level increases of pumping head, thus reducing the station efficiency and increasing the drainage cost, the settling of river and lagoon embankments reduces their freeboard.

Valle Isola and Valle Pega (Fig. 1) are the two basins mostly affected by land subsidence, with displacements amounting approximately to 2.5 cm in the southern portion and vanishing northward. Unsteady flow simulations have been performed in the present condition and in 2023 when the slope of the basins and the depth of the channel cross-sections have been updated in HEC-HMS and HEC-RAS, respectively, to account for the expected land subsidence.

The subsidence effects have been evaluated by comparing the two solutions in terms of water level and velocity in the channels, time behavior of the discharge at the closing sections, functioning of the pumping stations. The comparison points out that the differences are very small:

- the discharge hydrographs in the 2023 configuration are characterized by a faster development, with a difference of < 5 min. The maximum discharges remain almost unchanged;
- the maximum water velocity practically does not change;
- following the lowering of the channel beds, the profile of the

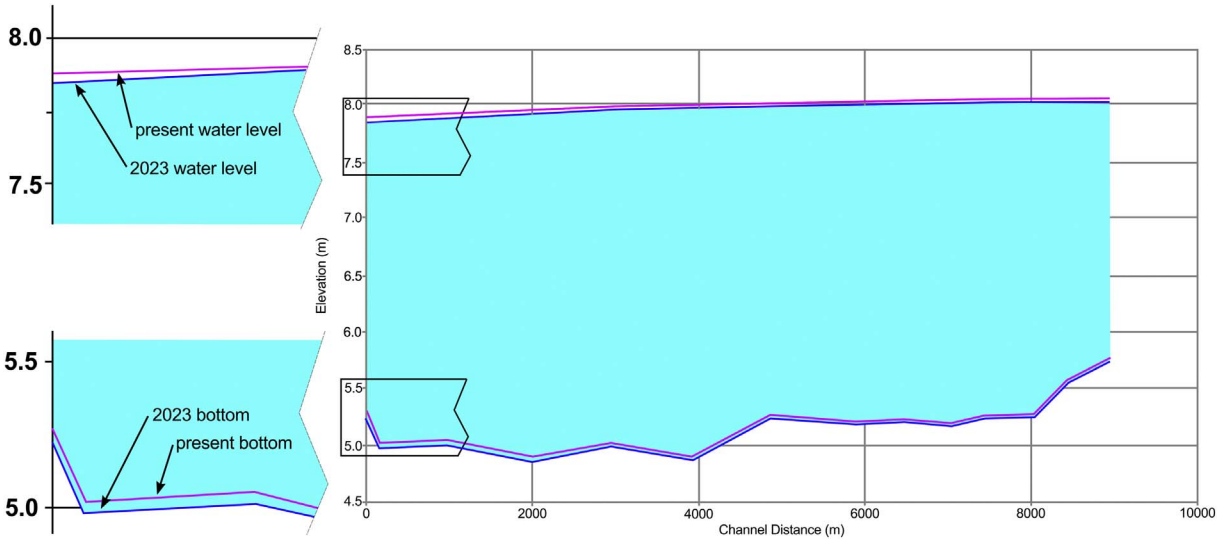

Fig. 13. Profiles of the bed and maximum water level along the main channel of the Valle Isola in the present condition and in 2023. The channel location is highlighted in Fig. 1.

maximum water level losses 1 to 2 cm in 2023 along the main channel of the Valle Isola and Valle Pega sub-basins (Fig. 13). No detectable difference is computed for the other sub-basins;

- the functioning rules of the pumping stations can remain unchanged because of the negligible variations of the water levels;
- the embankment freeboards does not change appreciably.

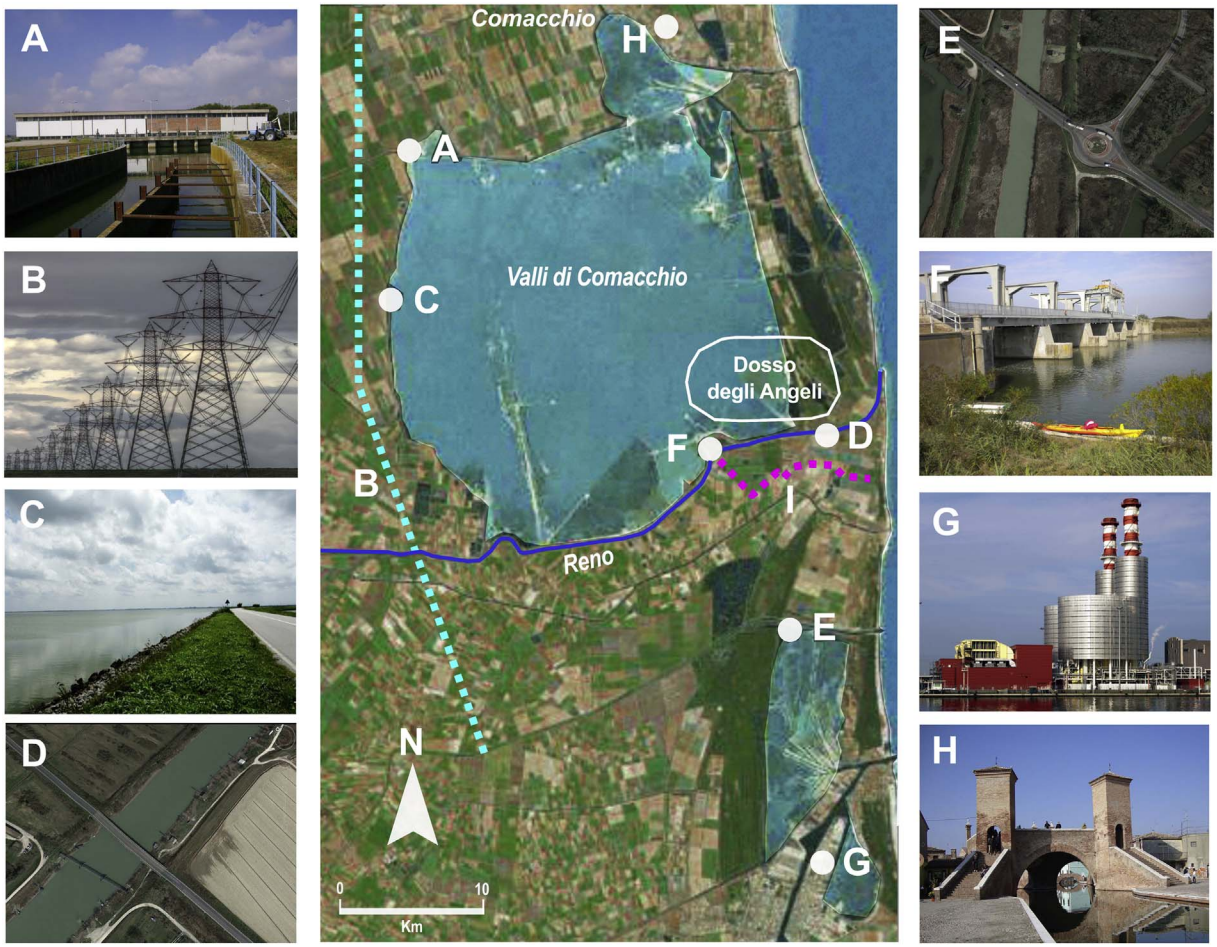

Fig. 14. Satellite image of the study area with the photo and location of the main structures and infrastructures: A) the Fosse pumping station; B) a major power-line crossing the territory from north to south; C) the Agosta embankment bounding the Comacchio Lagoons; D) the bridge on the State Road E55 crossing the Reno River; E) the bridge on the State Road E55 crossing the Lamone River; F) the mobile dam "Volta Scirocco" along the Reno River; G) the "Teodora" power plant; H) the "Trepponti di Comacchio" bridge; I). the "Mandriole" channel.

Table 2
Expected subsidence and displacement gradient due to the residual production from Dosso degli Angeli in correspondence of the main structures/infrastructures in the study area. The site locations are provided in Fig. 14.

Structure ID	Description	Subsidence 2013–2023 (cm)	ξ ($\times 10^{-6}$)
A	Fosse pumping station: main pumping station in the study area (length 70 m, maximum discharge 24 m^3/s)	1.1	6
B	Major power-line connecting the city of Ravenna to the main Porto Tolle power plant at the tip of the Po River delta	< 0.5	1–4
C	Agosta embankment: soil embankment bounding the Comacchio valleys (elevation: + 1.5 m above slm, i.e. + 4 m above the surrounding farmland)	< 2.8	2–6
D	Reinforced concrete bridge along the State Road E55 crossing the Reno river (length 115 m)	1.4	6
E	Reinforced concrete bridge along the State Road E55 crossing the Lamone river (length 140 m)	0.8	4
F	Volta Scirocco: tainter gate to control the water flow and level long the Reno river (5 mobile elements with a cumulative 125-m length)	0.9	2
G	Teodora thermal-power plant (capacity: 750 MW)	< 0.5	3
H	Trepponti di Comacchio: historical masonry bridge	2.6	3
I	Mandriole channel: infrastructure diverting water from the Reno river to supply the industrial aqueduct of the Ravenna industrial zone	0.9–1.9	4–5

6.2. Effects of the differential displacements on structures and infrastructures

Fig. 14 shows a map of the study area with the location of the main constructions and infrastructures. The displacement gradient that must be expected in these sites has been obtained using the results provided in Fig. 12.

A list with the characteristics of these structures and the computed ξ over the period 2013–2013 is provided in Table 2. The maximum displacement gradient is estimated at Fosse pumping station (site A), the nearby portion of the Agosta embankment (site C), and the bridge on the State Road E55 crossing the Reno River (site D), with a value equal to 6×10^{-6}. For the other constructions and infrastructures, ξ ranges from 1×10^{-6} to 5×10^{-6}. Comparing these values with the admissible bounds summarized in Table 1, it clearly emerges that neither static issues nor instrumentation (e.g., pump) malfunctioning are expected to occur, with ξ approximately 3 orders of magnitude smaller than the safety limits. Also for the Trepponti of Comacchio (site H), which is the most sensible masonry structure in the area, ξ is about 100 times below the 5×10^{-4} bound.

7. Discussion

Subsidence management is a key topic in several flat coastal areas worldwide. Key questions are: how much subsidence is acceptable and at which rate? How can it be reliably assured that (future) subsidence will stay within these limits? And, how can we split the cumulative values, provided for example by the SAR-based measurements, between the various processes contributing to the total subsidence amount?

Methodologies to try providing scientifically based answers to those questions are complex and not unique too, depending on the specific sites and the environmental topic to address. In the Netherlands, for example, where subsidence caused by extraction of hydrocarbons is an issue as sensitive as in Italy, the concept of "effective subsidence capacity" (de Waal et al., 2012) has been developed and is currently used to prevent damage to the tidal system in the Dutch Wadden Sea area. Generally speaking, the effective subsidence capacity is the maximum human-induced subsidence that the affected area can robustly sustain. Depending on the characteristics of the study area, the effective subsidence capacity can be defined in different terms, specifically a maximum subsidence volume, a maximum subsidence at a given location, or a maximum subsidence rate. In the Wadden Sea coastland, the long-term survival of the natural marsh system depends on its ability to keep balance with the average long-term relative sea-level rise by means of sedimentation and thus maintain a dynamic morphologic equilibrium. The limit of acceptable subsidence is the maximum rate of relative sea-level rise that can be accommodated in the long term with null impact in terms of coastal erosion and morphological deterioration. Note that a relative sea-level rise may be caused by either sea level-rise due to climate changes or not-climatic components such as land subsidence. The effective subsidence capacity available for human activities, such as gas production, is obtained by subtracting the expected average sea-level rise plus the natural subsidence from the limit of acceptable subsidence (i.e., the sedimentation rate in this specific case study). Modeling and monitoring are of paramount importance to develop reliable subsidence predictions and hence reliable application of the "effective subsidence capacity" concept.

Suggestions from the extensive legal, technical, and organizational framework in place in the Dutch country has been adapted to and applied in relation to the residual production from the Dosso degli Angeli reservoir located along the coast of the Adriatic Sea:

- during production, subsidence has been accurately measured in the field;

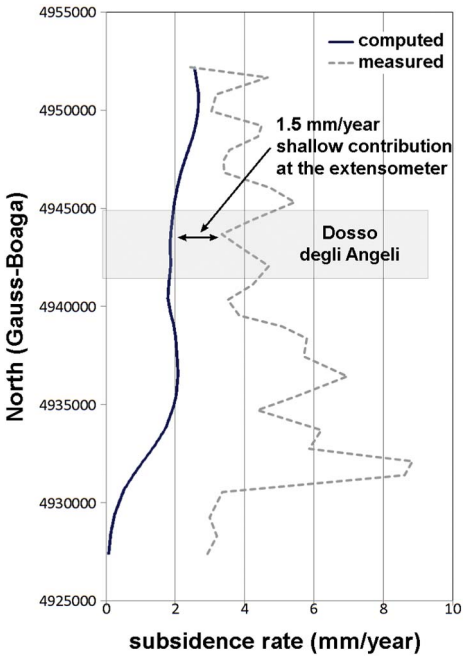

Fig. 15. Average subsidence rates (mm/year) along the shoreline of the study area due to the residual production from Dosso degli Angeli as computed by the FE model (Fig. 10) and measured between 2008 and 2011 using COSMO-SKYMED data (Fig. 6c), this latter reduced of the deep contribution estimated in 1.5 mm/year. The difference between the two profiles in correspondence of the north coordinate of the Dosso degli Angeli extensometer amounts to about 1.5 mm/year, in quite good agreement with the trend provided by the monitoring station (Fig. 5a). The difference between the "measured" and "computed" profiles is representative of the subsidence due to shallow processes (e.g., groundwater pumping, natural consolidation of compressible Holocene deposits, and compaction due to surficial loads).

- an advanced and integrated monitoring system has allowed quantifying the relative importance of the main processes contributing to the cumulative land subsidence;
- the subsidence due to hydrocarbon production has been simulated by an advanced 3D geomechanical model; the multi-decadal production life has allowed a reliable calibration of the model (Fig. 15);

- iv) the "effective subsidence capacity" has been identified for the study area. Because of the large land subsidence occurred in the past (Caputo et al., 1970; Teatini et al., 2005, 2006; Bitelli et al., 2010) and the complex sedimentary architecture of this coastland (Simeoni and Corbau, 2009), the main potential problems associated with land subsidence are located inland, i.e. in the lowlying farmland on the back of sandy coastal ridges and dune alignments. Therefore, the effective subsidence capacity corresponds to a lowering that does not reduce the efficiency of the reclamation system and does not mine the structural safety and instrumentation functioning of the major structures and infrastructures because of displacement gradients.

8. Conclusion

A three-dimensional finite-element modeling approach was used to predict the anthropogenic land subsidence expected at the northern Adriatic coastland due to the residual gas production planned from the Dosso degli Angeli field. The simulation time extends over 10 years, between 2013 and 2023, when the last 5% of the initial recoverable resource will be produced. The propagation of the pressure drawdown in the lateral/bottom aquifer was fully accounted for. The model, which was initially calibrated on a large dataset of subsidence and compaction measurements provided by levelling, CGPS, SqueeSAR, and extensometers, predicted a maximum subsidence and horizontal displacement equal to 2.8 cm and 2.0 cm, respectively. These values has allowed to evaluated an expected displacement gradients ranging between 10^{-6} and 10^{-5}, i.e. from 0.1 to 1 mm over 100 m.

The analyses presented in this work have been aimed at evaluating the impact of this man-induced process on the environment and structures/infrastructures beneath Dosso degli Angeli. The modeling investigations highlight that the anthropogenic land subsidence due to the residual gas production from this major gas reservoir is relatively small compared to the land subsidence recently measured in the area, with no practical consequence in terms of loss of efficiency of the reclamation network, increase of flooding hazard because of a freeboard reduction, and decrease of the structural safety caused by differential displacements.

Acknowledgments

The authors are much indebted to Eni for making available the data used in the present study.

References

Allison, M., Yuill, B., Törnqvist, T., Amelung, F., Dixon, T.H., Erkens, G., Stuurman, R., Jones, C., Milne, G., Steckler, M., Syvitski, J., Teatini, P., 2016. Global risks and research priorities for coastal subsidence. Eos 97. http://dx.doi.org/10.1029/2016EO055013.

d'Angremond, K., van de Water, J.P., 2012. Mining activities in a coastal zone. Effects and remedial measures in the Netherlands. In: Proc. of COPEDEC 2012, pp. 1085–1096.

Bartolini, C., Bernini, M., Carloni, G.C., Costantini, A., Federici, P.R., Gasperi, G., Lanzarotto, A., Marchetti, G., Mazzanti, R., Papani, G., Pranzini, G., Rau, A., Sandrelli, F., Vercesi, P.L., Castaldini, D., Francavilla, F., 1983. Carta neotettonica dell'Appennino Settentrionale. Note illustrative. Bollettino Società Geologica Italiana 101.

Baù, D., Ferronato, M., Gambolati, G., Teatini, P., 2002. Basin-scale compressibility of the Northern Adriatic by the radioactive marker technique. Geotechnique 52 (8), 605–616.

Bitelli, G., Bonsignore, F., Unguendoli, M., 2000. Levelling and GPS networks to monitor ground subsidence in the Southern Po Valley. J. Geodyn. 30, 355–369.

Bitelli, G., Bonsignore, F., Carbognin, L., Ferretti, A., Strozzi, T., Teatini, P., Tosi, L., Vittuari, L., 2010. Radar interferometry-based mapping of the present land subsidence along the low-lying northern Adriatic coast of Italy. In: Carreón-Freyre, D., Cerca, M., Galloway, D. (Eds.), Land Subsidence, Associated Hazards and the Role of Natural Resources Development, pp. 279–286 IAHS Publication no. 339.

Bjerrum, L., 1963. Allowable settlement of structures. In: Proc. European Conf. on Soil Mech. and Found. Engr., Weisbaden, Germany, vol. 3. pp. 135–137.

Bondesan, M., Castiglioni, G.B., Elmi, C., Gabbianelli, G., Marocco, R., Pirazzoli, P.A., Tommasin, A., 1995a. Coastal areas at risk from surges and sea-level rise in northeastern Italy. J. Coast. Res. 11 (4), 1354–1379.

Bondesan, M., Favero, V., Viñals, M.J., 1995b. New evidence on the evolution of the Po delta coastal plain during the Holocene. Quat. Int. 29/30, 105–110. http://dx.doi.org/10.1016/1040-6182(95)00012-8.

Bondesan, M., Simeoni, U., 1983. Dinamica e analisi morfologica statistica dei fondali del delta del Po e alle foci dell'Adige e del Brenta. Mem. Ist. Geol. e Min.. Padova 36, 1–48.

Buckley, S.M., Rosen, P.A., Hensley, S., Tapley, B.D., 2003. Land subsidence in Houston, Texas, measured by radar interferometry and constrained by extensometers. J. Geophys. Res. 108 (B11), 2542. http://dx.doi.org/10.1029/2002JB001848.

Caputo, M., Pieri, L., Unguendoli, M., 1970. Geometric investigation of the subsidence in the Po Delta. Boll. Geofis. Teor. Appl. 47, 187–207.

Carbognin, L., Gatto, P., G. Mozzi, 1984. Case history no.9.15: Ravenna, Italy, in: Poland J. F, Guidebook to Studies of Land Subsidence due to Ground-Water Withdrawal, U. N. Educ. Sci. and Cultural Organ., Paris, 291–305.

Carbognin, L., Teatini, P., Tosi, L., Strozzi, T., Tomasin, A., 2011. Present relative sea level rise in the Northern Adriatic coastal area. In: Brugnoli, E., Cavarretta, G., Mazzola, S., Trincardi, F., Ravaioli, M., Santoleri, R. (Eds.), Marine Research at CNR. Consiglio Nazionale delle Ricerche, Dipartimento Terra e Ambiente, pp. 1147–1162.

Carminati, E., Di Donato, G., 1999. Separating natural and anthropogenic vertical movements in fast subsiding areas: the Po plain (N. Italy) case. Geophys. Res. Lett. 26 (15), 2291–2294.

Carminati, E., Martinelli, G., 2002. Subsidence rates in the Po Plain, northern Italy: the relative impact of natural and anthropogenic causation. Eng. Geol. 66, 241–255.

Carreon-Freyre, D., Cerca, M., Ochoa-Gonzalez, G., Teatini, P., Zuñiga, F.R., 2016. Shearing along faults and stratigraphic joints controlled by land subsidence and hydraulic gradient in the Valley of Queretaro, Mexico. Hydrogeol. J. 24 (3), 657–674. http://dx.doi.org/10.1007/s10040-016-1384-0.

Chow, V.T., 1959. Open Channel Flow. McGraw-Hill, New-York, NY.

Colazas, X.C., Strehle, R.W., 1995. Subsidence in the Wilmington oil field, Long Beach, California, USA. In: Chilingarian, G.W., Donaldson, E.C., Yen, T.F. (Eds.), Subsidence due to Fluid Withdrawal. Elsevier Science, Amsterdam, pp. 285–335.

Da Deppo, L., Datei, C., Salandin, P., 2004. Sistemazione dei corsi d'acqua. Libreria Cortina Ed, Padova, Italy.

Douben, K.J., 2006. Characteristics of river floods and flooding: a global overview, 1985–2003. Irrig. Drain. 55, S9–S21.

Erban, L.E., Gorelick, S.M., Zebker, H.A., 2014. Groundwater extraction, land subsidence, and sea-level rise in the Mekong Delta, Vietnam. Environ. Res. Lett. 9, 084010. http://dx.doi.org/10.1088/1748-9326/9/8/084010.

Ferretti, A., Fumagalli, A., Novali, F., Prati, C., Rocca, F., Rucci, A., 2011. A new algorithm for processing interferometric data-stacks: SqueeSAR. IEEE T. Geosci. Remote Sens. 49. http://dx.doi.org/10.1109/TGRS.2011.2124465, 3460–3470.

Ferronato, M., Gambolati, G., Janna, C., Teatini, P., 2012. Modello di subsidenza antropica prodotta dalla coltivazione del giacimento di Dosso degli Angeli. Technical Report of the University of Padova (76 pp.).

Finol, A.S., Sancevic, Z.A., 1995. Subsidence in Venezuela. In: Chilingarian, G.W., Donaldson, E.C., Yen, T.F. (Eds.), Subsidence due to Fluid Withdrawal. Elsevier Science, Amsterdam, pp. 337–372.

Galloway, D., Riley, F.S., 1999. San Joaquin Valley, California: Largest human alteration of the Earths surface. In: Galloway, D., Jones, D.R., Ingebritsen, S.E. (Eds.), Land Subsidence in the United States, U.S. Geol. Surv. Circ. vol. 1182. U.S. Geol. Surv., Denver, Colorado, pp. 23–34.

Gambolati, G., Teatini, P., 1998. Numerical analysis of land subsidence due to natural compaction of the Upper Adriatic Sea basin. In: Gambolati, G. (Ed.), CENAS, Coastline Evolution of the Upper Adriatic Sea due to Sea Level Rise and Natural and Anthropogenic Land Subsidence. Kluwer Academic Publ., pp. 103–132 Water Science and Technology Library no. 28.

Gambolati, G., Teatini, P., 2015. Geomechanics of subsurface water withdrawal and injection. Water Resour. Res. 51, 3922–3955. http://dx.doi.org/10.1002/2014WR016841.

Gambolati, G., Ricceri, G., Bertoni, W., Brighenti, G., Vuillermin, E., 1991. Mathematical simulation of the subsidence of Ravenna. Water Resour. Res. 27 (11), 2899–2918.

Gambolati, G., Teatini, P., Tomasi, L., Gonella, M., 1999. Coastline regression of the Romagna region, Italy, due to natural and anthropogenic land subsidence and sea level rise. Water Resour. Res. 35 (1), 163–184.

Geertsma, J., 1973. Land subsidence above compacting oil and gas reservoir. J. Petr. Tech. 25, 734–744.

Hermansen, H., Landa, G.H., Sylte, J.E., Thomas, L.K., 2000. Experiences after 10 years of waterflooding the Ekofisk field, Norway. J. Pet. Sci. Eng. 26, 11–18.

Hoffmann, J., Galloway, D.L., Zebker, H.A., 2003. Inverse modeling of interbed storage parameters using land subsidence observations, Antelope Valley, California. Water Resour. Res. 37 (2), 1031. http://dx.doi.org/10.1029/2001WR001252.

Hueckel, T., Cassiani, G., Prevost, J.H., Walters, D.A., 2005. Field derived compressibility of deep sediments of North Adriatic. In: Barends, F.B.J., Carbognin, L., Gambolati, G., Steedman, R.S. (Eds.), Land Subsidence. Millpress, Rotterdam, the Netherlands, pp. 25–49 Special Volume.

Hung, W.-C., Hwang, C., Liou, J.-C., Lin, Y.-S., Yang, H.-L., 2012. Modeling aquifer-

system compaction and predicting land subsidence in central Taiwan. Eng. Geol. 147–148, 78–90.
Janna, C., Castelletto, N., Ferronato, M., Gambolati, G., Teatini, P., 2012. A geomechanical transversely isotropic model of the Po River basin using PSInSAR derived horizontal displacement. Int. J. Rock Mech. Min. Sci. 51. http://dx.doi.org/10.1016/j.ijrmms.2012.01.015, 105–118.
Mahmoudpour, M., Khamehchiyan, M., Nikudel, M.R., Ghassemi, M.R., 2016. Numerical simulation and prediction of regional land subsidence caused by groundwater exploitation in the southwest plain of Tehran, Iran. Eng. Geol. 201, 6–28.
Mattavelli, L., Ricchiuto, T., Grignani, D., Schoell, M., 1983. Geochemistry and habitat of natural gases in Po Basin, Northern Italy. AAPG Bull. 67 (12), 2239–2254.
Motagh, M., Shamshiri, R., Haghshenas Haghighi, M., Wetzel, H.U., Akbari, B., Nahavandchi, H., Roessner, S., Arabi, S., 2017. Quantifying groundwater exploitation induced subsidence in the Rafsanjan plain, southeasterner Iran, using InSAR time-series and in situ measurements. Eng. Geol. 218, 134–151.
Ng, A.H.-M., Ge, L., Li, X., Abidin, H.Z., Andreas, H., Zhang, K., 2012. Mapping land subsidence in Jakarta, Indonesia using persistent scatterer interferometry (PSI) technique with ALOS PALSAR. Int. J. Appl. Earth Obs. 18, 232–242.
Nicholls, R.J., Hoozemans, F.M.J., Marchand, M., 1999. Increasing flood risk and wetland losses due to global sea level rise: regional and global analyses. Glob. Environ. Chang. 9, 69–87.
Nicholls, R.J., Wong, P.P., Burkett, V., Woodroffe, C.D., Hay, J., 2008. Climate change and coastal vulnerability assessment: scenarios for integrated assessment. Sustain. Sci. 3, 89–102.
Ortiz-Zamora, D., Ortega-Guerrero, A., 2010. Evolution of long-term land subsidence near Mexico City: review, field investigations, and predictive simulations. Water Resour. Res. 46, W01513. http://dx.doi.org/10.1029/2008WR007398.
Pauw, P., de Louw, P.G.B., Oude Essink, G.H.P., 2012. Groundwater salinisation in the Wadden Sea area of the Netherlands: quantifying the effects of climate change, sea-level rise and anthropogenic interferences. Neth. J. Geosci. 91 (3), 373–383.
Ricceri, G., Soranzo, M., 1985. An analysis on allowable settlements on structures. Rivista Italiana di Geotecnica 4, 177–188.
Riley, F.S., 1986. Developments of borehole extensometry. In: Johnson, A.I., Carbognin, L., Ubertini, L. (Eds.), Land Subsidence. International Association of Hydrological Sciences Publication no. 151, 939 pp.
Rohmer, J., Raucoules, D., 2012. On the applicability of persistent scatterers interferometry (PSI) analysis for long term CO_2 storage monitoring. Eng. Geol. 147–148, 137–148.
Schlumberger Ltd, 2007. Eclipse technical description, report, v. 2007.1, Abingdon, U. K.Eclipse technical description, report, v. 2007.1, Abingdon, U. K.
Simeoni, U., Bondesan, M., 1997. The role and responsibility of man in the evolution of the Adriatic alluvial coasts of Italy. In: Briand, F., Maldonado, A. (Eds.), Transformations and evolution of the Mediterranean coastline. Science Series n° 3 18. Commission Internationale pour l'Exploration Scientifique de la mer Méditerranée (CIESM), pp. 111–132.
Simeoni, U., Corbau, C., 2009. A review of the Delta Po evolution (Italy) related to climatic changes ad human impacts. In: Corbau, C., Simeoni, U. (Eds.), Special Issue Coastal Vulnerability Related to Sea-Level Rise, Geomorphology. 107. pp. 64–71 issues 1–2.
Tamburini, A., Bianchi, M., Giannico, C., Novali, F., 2010. Retrieving surface deformation by PSInSAR technology: a powerful tool in reservoir monitoring. Int. J. Greenh. Gas Control 4, 928–937. http://dx.doi.org/10.1016/j.ijggc.2009.12.009.
Teatini, P., Ferronato, M., Gambolati, G., Bertoni, W., Gonella, M., 2005. A century of land subsidence in Ravenna, Italy. Environ. Geol. 47 (6), 831–846.
Teatini, P., Ferronato, M., Gambolati, G., Gonella, M., 2006. Groundwater pumping and land subsidence in the Emilia-Romagna coastland, Italy: modeling the past occurrence and the future trend. Water ResourRes. 42, W01406. http://dx.doi.org/10.1029/2005WR004242.
Todini, E., 1990. Indagine Statistica sulle piogge intense nel Comprensorio di Bonifica Renana. In: Technical Report. University of Bologna, Italy.
Tosi, L., Teatini, P., Carbognin, L., Brancolini, G., 2009. Using high resolution data to reveal depth-dependent mechanisms that drive land subsidence: the Venice coast, Italy. Tectonophysics 474, 271–284.
USACE-HEC, 2010. Hydrologic Modeling System, HEC-HMS v3.5 - User's Manual. US Army Corps of Engineers, Hydrologic Engineering Center Tech. Report CPD-74A.
USACE-HEC, 2016. River Analysis System, HEC-RAS v5.0 - User's Manual. US Army Corps of Engineers, Hydrologic Engineering Center Tech. Report CPD-68.
Viggiani, C., 2003. Fondazioni. Helvelius Edizioni, Benevento, Italy.
de Waal, J.A., Roest, J.P.A., Fokker, P.A., Kroon, I.C., Breunese, J.N., Muntendam-Bos, A.G., Oost, A.P., van Wirdum, G., 2012. The effective subsidence capacity concept: how to assure that subsidence in the Wadden Sea remains within defined limits? Neth. J. Geosci. 91 (3), 385–399.
Wu, J., Shi, X., Xue, Y., Zhang, Y., Wei, Z., Yu, J., 2008. The development and control of the land subsidence in the Yangtze Delta, China. Environ. Geol. 55 (8), 1725–1735.
Wu, J., Shi, X., Ye, S., Xue, Y., Zhang, Y., Wei, Z., Fang, Z., 2010. Numerical simulation of viscoelastoplastic land subsidence due to groundwater overdrafting in Shanghai, China. J. Hydrol. Eng. 15 (3), 223–236.
Zanello, F., Teatini, P., Putti, M., Gambolati, G., 2001. Long term peatland subsidence: Experimental study and modeling scenarios in the Venice coastland. J. Geophys. Res. 116, F04002. http://dx.doi.org/10.1029/2011JF002010.
Zhu, L., Gong, H., Li, X., Wang, R., Chen, B., Dai, Z., Teatini, P., 2015. Land subsidence due to groundwater withdrawal in the northern Beijing plain, China. Eng. Geol. 193, 243–255.